ISSN 0965-5425, Computational Mathematics and Mathematical Physics, 2015, Vol. 55, No. 2, pp. 317–329. © Pleiades Publishing, Ltd., 2015.
Original Russian Text © A.O. Antonova, T.I. Savyolova, 2015, published in Zhurnal Vychislitel'noi Matematiki i Matematicheskoi Fiziki, 2015, Vol. 55, No. 2, pp. 322–334.

Error Estimation for Computed Polycrystalline Texture Characteristics by Varying Measurement Parameters in Electron Microscopy Methods

A. O. Antonova and T. I. Savyolova

Moscow Engineering Physics Institute (State University), Kashirskoe sh. 31, Moscow, 115409 Russia
e-mail: aoantonova@mail.ru, tisavelova@mephi.ru

Received June 24, 2014

Abstract—A two-dimensional mathematical model is proposed for a polycrystalline specimen and an electron microscopy experiment with varying measurement parameters, such as the scanning step and the threshold disorientation angle. Experimental results are used to compare specimen texture characteristics and measurements: the grain size distribution, average grain size, variance; disorientation angle distribution, average disorientation angle, variance; and estimates of the orientation distribution function in three-dimensional form in a one-parameter representation. All these distributions are tested by applying a chi-square homogeneity test. The most important aspects of the experiment are formulated as propositions.

DOI: 10.1134/S0965542515020025

Keywords: orientation on the rotation group $SO(3)$, Monte Carlo method, grain size distribution density, disorientation angle distribution density, orientation distribution function, measurement step, threshold disorientation angle, chi-square test.

INTRODUCTION

Recent advances in electron back scattering diffraction (EBSD) [1–4] have opened up new opportunities in the study of material structure and texture. Together with determining grain sizes, EBSD has provided a simple and quick tool for receiving information on the texture and character of grain boundaries in material structures. It is these structure characteristics that determine, in many respects, the physical and mechanical properties and mechanisms of texture formation (plastic deformations, phase transitions, recrystallization, etc.) [5–8].

The goal of EBSD analysis is also to study the spatial orientation distribution. Due to the large number of orientations in the material under study, the orientation distribution function (ODF) can be calculated without measuring polar figures (PFs) by X-ray or other methods [9]. PFs can also be calculated directly from orientations. ODFs are used to examine the physical (thermal, elastic, plastic, etc.) properties of materials.

The accuracy of ODF recovery from a set of individual orientations depending on the sample size and smoothing parameters were studied in [10–15].

Before conducting EBSD measurements, an experimenter has to prepare a specimen and specify a measurement step and a disorientation angle in order to distinguish grains with different orientations. The problem of choosing measurement parameters remains insufficiently investigated, while these parameters have a large effect on measurement results. In a number of works (see [2, 10, 16–18]), it was indicated than an unsuitable choice of measurement parameters leads to incorrect results. For example,

an insufficient number of orientation measurements results in low accuracy of computed PFs (see [10]);

disorientation angle measurements may lead to inconsistent average grain size values (see [16]);

a small step of measurements leads to a considerable increase in time required for conducting an experiment (see [17, 18]).

We can say that the development of experimental technology outruns the mathematical apparatus of processing electron microscopy data. In [19] the formation of material structure and texture was investigated using real-time electron microscopy methods. Accordingly, it is of interest to study this issue with the help of the mathematical simulation of an experiment.

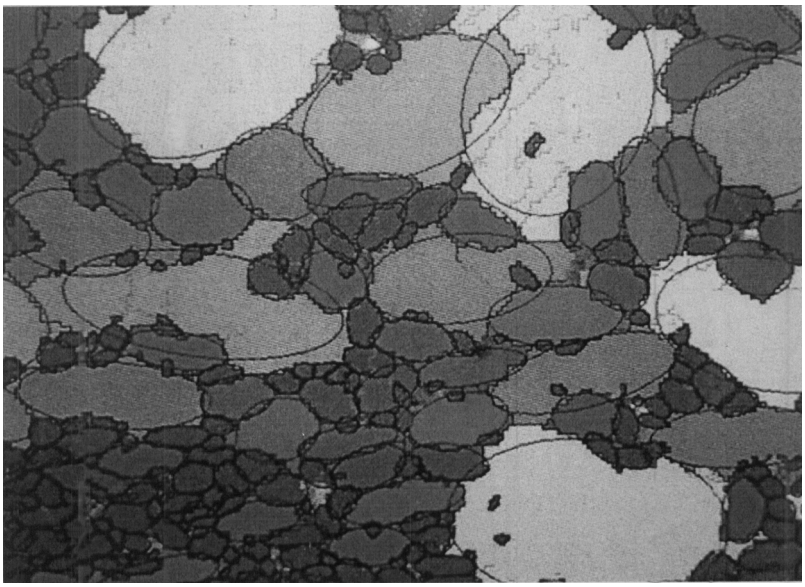

Fig. 1. Example of the approximation of grain cross sections by ellipses.

Below, we develop a two-dimensional mathematical model of a specimen and a subsequent EBSD experiment. The specimen represents a set of grains, each having its own size, orientation, and disorientation angles with neighboring grains. Orientations are simulated by applying a special Monte Carlo method [20, 21]. The grain size distribution is assumed to be given. Specimen measurements are modeled for various experiment parameters. The experimental results are used to compare specimen texture characteristics and measurements: the grain size distribution, average grain size, variance; the disorientation angle distribution, average disorientation angle, variance; and ODF estimates in three-dimensional form in a one-parameter representation. The coincidence of all these distributions is tested by applying a chi-square homogeneity test [22].

1. PRELIMINARIES

In this study, the rotation of a grain is described by the Euler angles $g = \{\varphi, \theta, \psi\}$, where $-\pi \le \varphi, \psi \le \pi$ and $0 \le \theta \le \pi$, and by corresponding rotation matrix from the group $SO(3)$ (see [9]).

Inverse rotation can be written as $g = \{\pi - \psi, \theta, \pi - \varphi\}$. In what follows, by the *orientation of a grain*, we mean the corresponding element $g \in SO(3)$.

A polycrystalline specimen consisting of grains with various sizes and orientations is treated as a statistical object. For its mathematical description, we use the following characteristics:

(i) the grain size distribution density (GSDD);

(ii) the disorientation angle distribution density (DADD) between neighboring grains;

(iii) the orientation distribution function (ODF).

In the commercial software [23], the plane cross sections of grains are approximated by circles whose diameters are written as grain sizes (Fig. 1).

The disorientation angles g_i and g_{i+1} ($i = 1, \ldots, N-1$) between two neighboring grains are calculated using the formula (see [9])

$$\cos\omega_i = \frac{\mathrm{Tr}(g_i g_{i+1}^{-1}) - 1}{2}, \quad 0 \le \omega_i \le \pi, \quad i = 1, \ldots, N-1. \tag{1.1}$$

The DADD is the distribution density of the angles ω_i, $i = 1, \ldots, N-1$.

In the general case, the ODF is a function on $SO(3)$ that can be expanded in the series (see [12–15])

$$f(g) = \sum_{l=0}^{\infty} \sum_{m,n=-l}^{l} C_{mn}^{l} T_{mn}^{l}(g), \tag{1.2}$$

where $T_{mn}^{l}(g)$ are the generalized spherical functions of the first order.

If the texture is described by a central normal distribution (CND), the expansion coefficients C_{mn}^{l} can be represented as

$$C_{mn}^{l} = (2l+1)\exp\{-l(l+1)\varepsilon^2\}\delta_{mn}, \tag{1.3}$$

where ε is a parameter characterizing the sharpness of the texture.

In view of (1.2) and (1.3), the CND can be written analytically as

$$f(t) = \sum_{l=0}^{\infty}(2l+1)\exp\{-l(l+1)\varepsilon^2\}\frac{\sin\left(l+\frac{1}{2}\right)t}{\sin\frac{t}{2}}, \quad t\in[-\pi;\pi], \tag{1.4}$$

$$\cos\frac{t}{2} = \cos\frac{\varphi+\psi}{2}\cos\frac{\theta}{2}.$$

In [20, 21] a special Monte Carlo method was developed that calculates CND (1.4) as a set of individual orientations on $SO(3)$. This method was used in [9, 12–15] to model EBSD measurements and smooth out ODFs.

The kernel ODF estimator has the form

$$f_N(g) = \frac{1}{(\alpha)^3}\sum_{i=1}^{N}C_i q_1\left(\frac{\varphi-\varphi_i}{\alpha}\right)q_3\left(\frac{\psi-\psi_i}{\alpha}\right)q_2\left(\frac{\cos\theta-\cos\theta_i}{\alpha}\right), \quad C_i = \frac{x_i}{\sum_{i=1}^{N}x_i}, \tag{1.5}$$

where $C_i > 0$ ($i = 1, \ldots, N$) are weights determined by the grain sizes and $g_i(t)$ ($i = 1, 2, 3$) are smoothing kernels (see [9]).

2. CARRYING OUT A MODEL EXPERIMENT

2.1. Modeling of a Specimen

A specimen is a set of grains

$$\{(x_i, g_i, \omega_i), i = 1, 2, \ldots, N-1, (x_N, g_N)\}, \tag{2.1}$$

where x_i is the size of the ith grain, which is equal to the diameter of a circle whose area is equal to that of the grain's cross section; $g_i = (\varphi_i, \theta_i, \psi_i)$ is the orientation of the ith grain corresponding to the Euler angles $-\pi \le \varphi_i, \psi_i < \pi$ and $0 \le \theta_i \le \pi$; $\omega_i = (g_i, g_{i+1})$ is the disorientation angle between neighboring grains; and N is the number of grains in the specimen.

Following the Neumann method [24], grain sizes are chosen as random variables distributed satisfying a gamma distribution of the form (see [10])

$$p(x, a, b) = \frac{b^a}{\Gamma(a)}x^{a-1}e^{-bx}, \quad x \ge 0, \quad a > 0, \quad b > 0, \tag{2.2}$$

with expectation a/b and variance a/b^2.

A set of grain orientations with a distribution function in the form of CND with a given parameter $\varepsilon > 0$ is generated by the special Monte Carlo method with the number of convolutions equal to $n = 6$.

The specimen modeling results are presented in the following form:

(i) the distribution histogram over the grain sizes x_i, $i = 1, \ldots, N$;

(ii) ODF estimator (1.5), where

$$C_i = \frac{x_i}{\sum_{i=1}^{N}x_i};$$

(iii) the DADD histogram over the disorientation angles ω_i, $i = 1, \ldots, N-1$.

It is well known that a histogram is an unbiased and consistent estimator of the distribution density as $N \longrightarrow \infty$, $h_N \longrightarrow 0$ (the size of a column where the density is considered a constant), and $Nh_N \longrightarrow \infty$ (see [25]).

A specimen with boundaries is a set of grains (2.1) separated by boundaries, which are variables uniformly distributed in $[0, 2\gamma/10)$, where $\gamma > 0$ is such that the area of the boundaries is 10% of the grains' area. The area of a domain with measurement boundaries usually amounts to 10 to 50% (see [17, 18]).

2.2. Modeling of Specimen Measurements

The following measurement parameters are specified:

h is the scanning step, and ω_0 is a threshold disorientation angle for determining two different neighboring grains g_i and g_{i+1} from the disorientation angle (1.1) between them.

Measurements are made at the points $\Delta_k = kh$, $k = 1, 2, ..., N_1$. A measurement at the point $\Delta_1 = h$ is made using the orientation of the grain that contains the point Δ_1 (the resulting orientation is denoted by $\hat{g}_1$); for the point $\Delta_2 = 2h$, the next orientation $\hat{g}_2$ is determined, etc. In the case of a specimen with boundaries, if the point hits the boundary, it is assigned an orientation corresponding to the Euler angles equal to the arithmetic mean of the angles of two nearest determined orientations.

The resulting orientations are used to calculate the disorientation angles $\hat{\omega}_k = (\hat{g}_k, \hat{g}_{k+1})$, $k = 1, ..., N_1 - 1$, with the help of formula (2.3). If $\hat{\omega}_k \le \omega_0$, then the kth and $(k+1)$th steps belong to a single grain; i.e., the distance $((k-1)h, (k+1)h)$ lies inside a single grain. If n measurements are inside the jth grain, then the grain size is set equal to $\tilde{x}_j = nh$ and the Euler angles are calculated as the arithmetic mean of the corresponding n measurements:

$$\tilde{\varphi}_j = \frac{1}{n}\sum_{i=1}^{n}\hat{\varphi}_{ji}, \quad \tilde{\theta}_j = \frac{1}{n}\sum_{i=1}^{n}\hat{\theta}_{ji}, \quad \tilde{\psi}_j = \frac{1}{n}\sum_{i=1}^{n}\hat{\psi}_{ji}.$$

If $\hat{\omega}_k > \omega_0$, then a new grain begins at the point $(k+1)h$.

As a result of the measurements, we obtain a set of grains

$$\{(\tilde{x}_i, \tilde{g}_i, \tilde{\omega}_i), i = 1, 2, \ldots, \tilde{N} - 1, (\tilde{x}_{\tilde{N}}, \tilde{g}_{\tilde{N}})\}. \tag{2.3}$$

The experimental results are processed by constructing a histogram of the grain sizes $\tilde{x}_i$, $i = 1, 2, ..., \tilde{N}$, computing an ODF estimator similar to (1.5), and constructing a histogram of DADD $\tilde{\omega}_i$, $i = 1, 2, ..., \tilde{N} - 1$.

3. PROCESSING OF EXPERIMENTAL RESULTS

Assuming that ODF (1.5), DADD, and GSDD of the specimen are known, the numerical results produced in the modeling experiment can be compared with specimen data.

We calculate estimators of GSDD and DADD, namely, the expectations $M\xi$, $M\omega$ and the variances $D\xi$, $D\omega$ for the specimen and measurements:

$$\bar{x} = \sum_{i=1}^{N} x_i, \quad \bar{\omega} = \sum_{i=1}^{N} \omega_i;$$

$$\bar{\tilde{x}} = \sum_{i=1}^{\tilde{N}} \tilde{x}_i, \quad \bar{\tilde{\omega}} = \sum_{i=1}^{\tilde{N}} \tilde{\omega}_i;$$

$$s^2 = \frac{1}{N-1}\sum_{i=1}^{N}(x_i - \bar{x})^2, \quad s^2 = \frac{1}{N-2}\sum_{i=1}^{N-1}(\omega_i - \bar{\omega})^2;$$

$$s^2 = \frac{1}{\tilde{N}-1}\sum_{i=1}^{\tilde{N}}(\tilde{x}_i - \bar{\tilde{x}})^2, \quad s^2 = \frac{1}{\tilde{N}-2}\sum_{i=1}^{\tilde{N}-1}(\tilde{\omega}_i - \bar{\tilde{\omega}})^2.$$

The hypothesis that the actual and observed GSDD and DADD coincide is checked using a chi-square homogeneity test. For this purpose, we use the statistic (see [22])

$$Z = N\tilde{N}\sum_{j=1}^{r}\frac{\left(\frac{m_j}{N}-\frac{\tilde{m}_j}{\tilde{N}}\right)^2}{m_j+\tilde{m}_j},$$

where r is the number of cells in the partition, m_j and $\tilde{m}_j$ are the numbers of grains within the jth cell in the specimen and measurements, respectively. In each case, the range of grain sizes was partitioned so that the frequencies of grains hitting an individual cell for the specimen and measurements were as close as possible.

The chi-square homogeneity test was also used to check the coincidence of the one-parameter ODF representations for the specimen and measurements, which are given by the formula (see [9])

$$f_N(t) = \frac{1}{\alpha}\sum_{i=1}^{N} C_i q\left(\frac{t-t_i}{\alpha}\right), \quad C_i = \frac{x_i}{\sum_{i=1}^{N} x_i}, \tag{2.4}$$

$$t \in [-\pi, \pi], \cos\frac{t}{2} = \cos\frac{\varphi+\psi}{2}\cos\frac{\theta}{2},$$

where $q(t)$ is a Gaussian smoothing kernel.

For ODF measurements, the orientations and grain sizes that were obtained as a result of experiment are used in formula (2.4).

4. NUMERICAL RESULTS

4.1. Results for Specimens without Boundaries

Following the scheme described in Subsection 2.1, we modeled two specimens with the following gamma distribution parameters:

(1) $a = 2$ and $b = 1$; then $M\xi = a/b = 2$ is the average grain size in a specimen and $D\xi = a/b^2 = 2$;

(2) $a = 8$ and $b = 2$; then $M\xi = a/b = 4$ is the average grain size in a specimen and $D\xi = a/b^2 = 2$.

A chi-square test was used to check whether the gamma distribution coincides with the distribution of the resulting specimen grain sizes. The coincidence hypothesis was accepted at 95% confidence level. The value of the statistic was found to be 3×10^{-5} with 50 degrees of freedom.

The number N of grains in a specimen was set equal to 1000. The grain orientations in a specimen were modeled by the special Monte Carlo method for CND on $SO(3)$ with texture sharpness $\varepsilon = 1/8$ and with the number of convolutions equal to $n = 6$ (see [9]).

Next, the experiment model proposed in Subsection 2.2 was used. The following measurement parameters were chosen for a given specimen:

(a) $h = 0.5$ μm, 1.0 μm, 2.0 μm for specimen (1), $h = 2.2$ μm, 3.0 μm, 4.0 μm for specimen (2);

(b) $\omega_0 = 5°$, 10°, and 20°.

The scanning steps for the specimens were chosen so that the number of grains in with sizes smaller than the step one specimen was approximately equal to that in the other.

Since the specimens were measured entirely, the number of measured grains in each specimen was 1000.

Below, the results and recommendations concerning the choice of EBSD measurement parameters are given in the form of propositions.

Proposition 1. *If the scanning step is equal to h, then the fraction δ_{less_h} of grains whose sizes are less than h has to be taken into account.*

If the scanning step $h = 0.5$, 1.0, or 2.0 μm is chosen for specimen (1), then, taking into account only the average grain size in the specimen, we would have to choose $h = 4.0$, 2.0, or 1.0 μm, respectively, for specimen (2). However, for specimen (2), results similar to those for specimen (1) at $h = 0.5$ μm or even somewhat better are obtained even with the scanning step $h = 2.2$ μm. Note that $h = 0.5$ μm for specimen (1) and $h = 2.2$ μm for specimen (2) correspond to the same fraction of grains with sizes smaller than the scanning step (see Table A.3 in the Appendix). It is also worth noting that, choosing $h = 2.2$ μm rather than

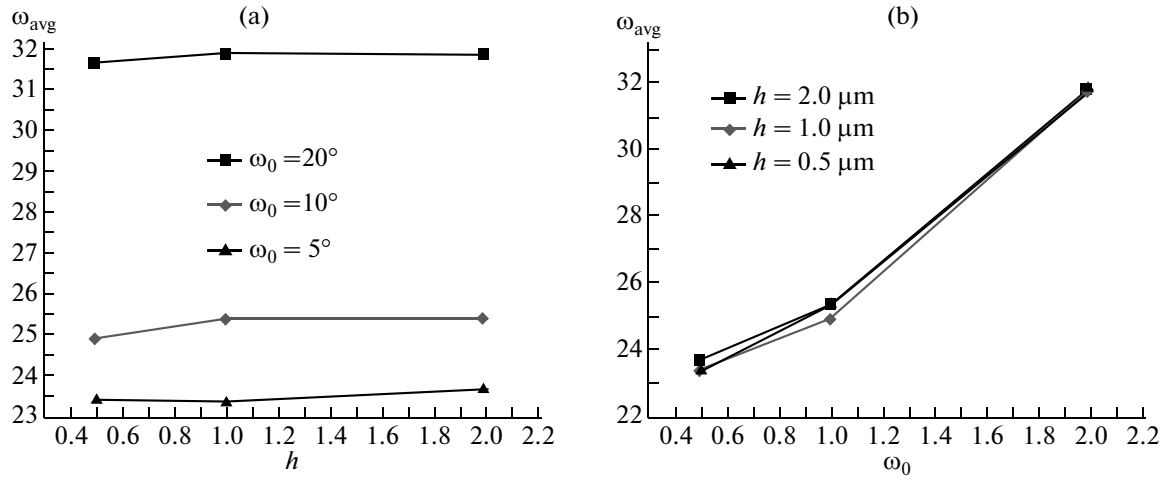

Fig. 2. Average disorientation angle as a function of the (a) measurement step and (b) threshold disorientation angle.

$h = 1.0$ μm, the experimenter can obtain a larger statistical sample over the same time. It was shown in [11, 12] that the sample size plays an important role in ODF recovery from a set of individual orientations.

Proposition 2. *The average disorientation angle and the DADD variance are strongly affected by the threshold disorientation angle and are weakly affected by the scanning step* (<0.5°).

Figure 2 shows the results obtained for specimen (1). The results for specimen (2) are nearly similar.

Proposition 3. *According to the chi-square homogeneity test, the hypothesis on the coincidence of the GSDD, DADD, and ODF for the specimen and measurements is accepted at* 95% *confidence level for small* $\omega_0 = 5°$ *and for the steps* $h = 0.5$, 1.0 μm *and* $h = 2.2$, 3.0 μm *for specimens* (1) *and* (2), *respectively.*

It should be noted that the hypothesis on the coincidence of DADD for the specimen and measurements is accepted at 95% confidence level only for small $\omega_0 = 5°$ regardless of the considered steps. This finding is explained by the fact that both specimens are strongly textured (have a texture of sharpness $\varepsilon = 1/8$) so, for the grains and DADD to be determined more accurately, we need to choose a smaller threshold disorientation angle. In the general case, the threshold disorientation angle has to be chosen taking into account the method of obtaining the specimen under study.

The hypothesis on the coincidence of GSDD is rejected when the scanning step id on the order of the average grain size in the specimen and/or the threshold disorientation angle is equal to 20°. In the other cases, the hypothesis is accepted at 95% confidence level.

The hypothesis on the coincidence of the one-parameter ODFs is rejected at $\omega_0 = 20°$ (in this case, the ODFs oscillate on the "tails" and the maxima increase). In the other cases, it is accepted at 95% confidence level. For three-dimensional ODFs at $\omega_0 = 20°$ and, in some cases, for $\omega_0 = 10°$, the maximum is observed to increase (Fig. 3a), but the coordinates of the maximum remain nearly unchanged. This behavior of the ODF is similar to that in the presence of dependent orientations [9], which arise at $\omega_0 = 20°$ because of merging a large number of grains.

Proposition 4. *In the cased of strongly textured specimens, the ODF should be recovered with a small threshold disorientation angle.*

For the specimens under consideration, as such an angle, we can use $\omega_0 = 5°$.

Proposition 5. *A decrease in the scanning step insignificantly improves the ODF recovered from individual orientations.*

At the same time, the statistical sample is reduced substantially. For more detail on the effect of a sample on ODFs recovered from individual orientations, see [11, 12].

Some more remarks have to be made about the scanning step. To obtain more accurate shapes and sizes of grains, the step is usually chosen to be 1/10–1/5 times as large as the average grain size in the specimen (see [6–8, 11]). This step corresponds to $\delta_{less\_h} < 5\%$ (see Table A.3 in the Appendix). However, this step

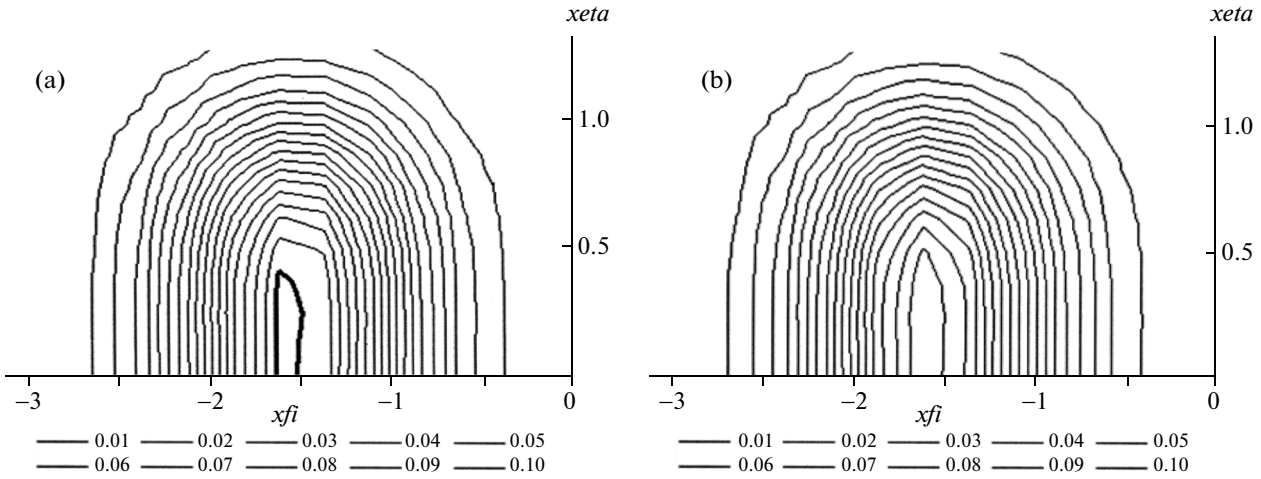

Fig. 3. Contour lines of ODF cross section for (a) $h = 0.5$ μm, $\omega_0 = 20°$ and (b) for specimen (1).

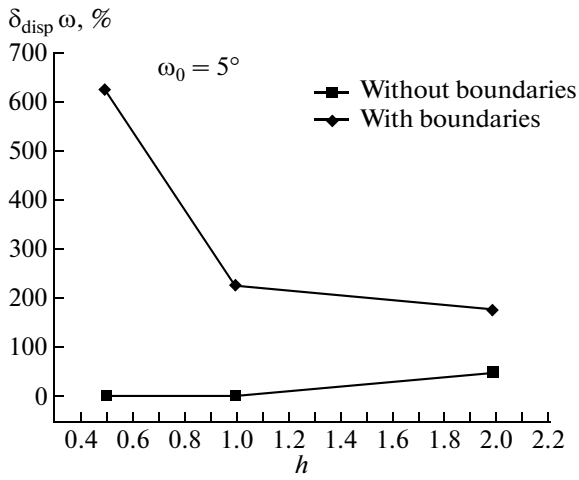

Fig. 4. Relative error of the DADD variance as a function of h.

may be unsuitable for ODF recovery. With respect to many parameters, such as GSDD, DADD, anf the homogeneity test for them and ODF, acceptable results are obtained even with a step corresponding to $\delta_{less\_h} \approx 25\%$. In this case, the sample turns out to be several times as large.

4.2. Results for Specimens with Boundaries

As a specimen with boundaries, we examined (1) with boundaries added as described in Subsection 2.1.

The following observations were made by measuring the new specimen, in which the boundaries amount to about 10% of the total grain size $\gamma = \bar{x}$.

In the experiment, we measured part of the specimen with boundaries that was equal to the specimen without boundaries, so 912 grains were examined.

Proposition 6. *As the scanning step decreases, the number of hits on the boundaries increase.*

Table A.2 gives the number of found grains.

Here, n_{bound} is the number of hits on the grain boundaries in measurement.

Table 1

$Mx = 2.033$			
h, μm	ω_0		
	20°	10°	5°
2.0	5.067	3.084	2.728
1.0	4.296	2.496	**2.110**
0.5	3.893	**2.121**	1.689

Proposition 7. *When the point hits a grain boundary, the corresponding orientation found as the arithmetic mean of two neighboring ones can form an individual grain* (*which is referred to as imaginary*).

Thus, such an orientation differs from both neighboring ones by an angle larger than ω_0. In Table A.2, the number of such orientations in each case is indicated in parentheses. As ω_0 decreases, they become more abundant. As the scanning step decreases, the total number of hits on grain boundaries grows and, as a result, the number of imaginary grains increases as well.

Corollary to Proposition 7. The presence of imaginary grains strongly distorts the results, and the distortions are larger for smaller values of h and ω_0.

This is especially evident in the variance of grain sizes and disorientation angles (Tables A.6 and A.8). A visual illustration of the degradation in the results can be seen in Fig. 4, which shows the relative error of the DADD variance for a small angle. It can be seen that, as the step decreases for small ω_0, the error increases sharply for the specimen with boundaries, while, for the specimen without boundaries, it tends to zero.

Since more grains of small sizes appear, the average grain size is reduced (Table 1). The results closest to the average grain size in the specimen are shown in bold.

It can be seen that they either correspond to the "medium-sized" step $h = 1.0$ μm (since the imaginary grains seem to be still rather few for this step size) or to a small-sized step, but for a moderate value of ω_0. In the latter case, the step is small enough for frequent hits on boundaries (hence, many imaginary grains can appear), but at $\omega_0 = 10°$ the formation of imaginary grains is less frequent than for a smaller threshold disorientation angle. It can be assumed that the results of [16] on obtaining the average grain size in a specimen can be explained in a similar manner. For a scanning step that is 1/10–1/5 times as large as the average grain size in the specimen, the best results were obtained for $\omega_0 = 11°$, 12°. Possibly, for the specimen

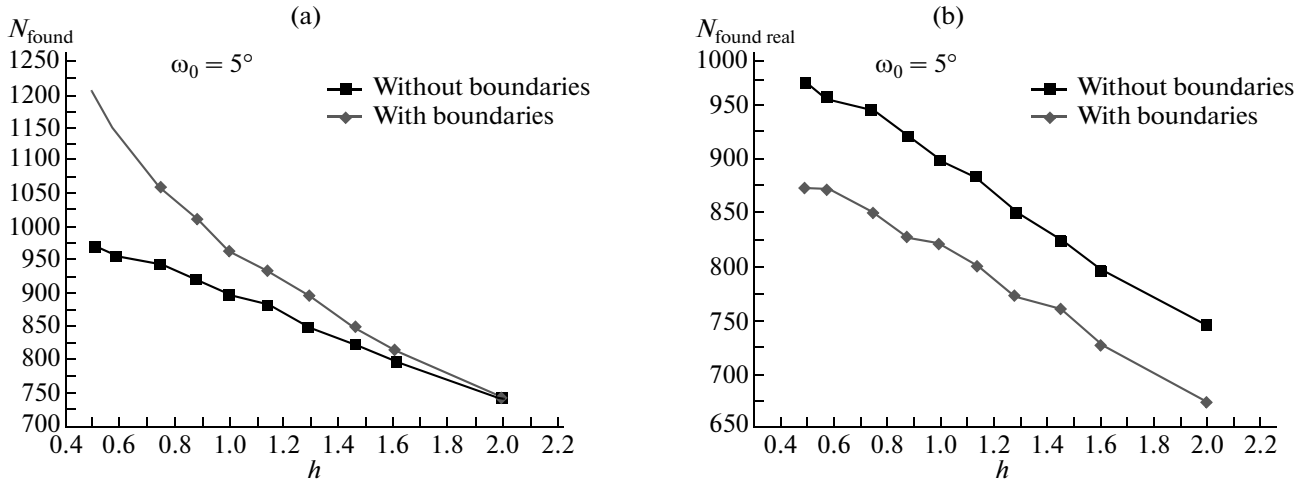

Fig. 5. The number of found grains vs. the scanning step (a) with and (b) without allowance for imaginary grains.

examined in [16], these threshold disorientation angles prevented the formation of a large number of imaginary grains, which would have a large effect on the results.

The deterioration of the results is manifested by the chi-square homogeneity test. For GSDD and DADD, the test is not satisfied for the smallest of the considered steps. For ODF the values of the statistic in the test increase by several times, but they satisfy the chi-square homogeneity test at 95% confidence level in the same cases as for the specimen without boundaries.

Some results with explanations are given in the Appendix. For example, the relative errors of the average grain sizes in specimens with and without boundaries are compared at identical numbers of grains with a size less than the step. Additionally, the numbers of grains found for specimens with and without boundaries and the number of hits on the boundary in the course of measurements are given.

The following observation has to be noted. Figure 5a shows the total number of found grains as a function of the scanning step for specimens with and without boundaries, while, in Fig. 5b, the imaginary grains were eliminated from the total number of found grains for the specimen with boundaries. It can be seen that, without imaginary grains, the dependence has a similar character.

CONCLUSIONS

A two-dimensional mathematical model of a specimen and an EBSD experiment was developed for various measurement parameters, such as the scanning step and the threshold disorientation angle. It was shown that the latter has a large effect on the measurement results. This angle has to be chosen taking into account the specimen-manufacturing method. For a high percentage of boundaries in a specimen, a too small scanning step may lead to distortions of the results due to the formation of imaginary grains. To obtain more accurate results, a scanning step has to be chosen taking into account not only the average grain size in the specimen, but also use, if possible, some additional information on the grain size variance, for example, the fraction of grains in a specimen with a size smaller than the step.

It should be noted that EBSD measurements deal only with a thin surface layer of a specimen (see [1, 2]). The computation of ODF requires that a large number of orientations be processed [10]. For this reason, a 3D representation of a specimen in terms of two-dimensional map measurements has been used progressively more frequently at present (see [6, 9]).

APPENDIX

Number $N_{\text{found gr}}$ of Grains Found in the Experiment

- h is the measurement step, ω_0 is the threshold disorientation angle;
- $\delta_{\text{less } h}$ is the fraction of specimen grains smaller than h in size.

The cases analyzed in detail are shown in bold.

Table A.1

$\delta_{\text{less } h}$, %	Specimen (1)			Specimen (2)		
	h, μm	$N_{\text{found gr}}$, $\omega_0 = 5°$	$N_{\text{found gr}}$, $\omega_0 = 10°$	h, μm	$N_{\text{found gr}}$, $\omega_0 = 5°$	$N_{\text{found gr}}$, $\omega_0 = 10°$
57	**2.00**	**741**	**682**	**4.00**	**840**	**770**
45	1.61	795	731	3.54	883	805
40	1.46	824	752	3.38	905	812
35	1.29	849	777	3.24	917	844
30	1.14	883	808	3.09	929	848
25	**1.00**	**898**	**823**	**3.00**	**935**	**856**
20	0.88	920	842	2.70	961	877
15	0.75	944	865	2.52	967	884
10	0.58	957	873	2.30	975	891
8	**0.50**	**970**	**890**	**2.20**	**978**	**895**

• n_{bound} is the number of hits on grain boundaries in the measurement.

The number of imaginary grains is given in parentheses.

Table A.2

$\delta_{\text{less }h}$, %	h, μm	Specimen (1) with boundaries (912 grains measured)			Specimen (1) (1000 grains measured)	
		$N_{\text{found gr}}$, $\omega_0 = 5°$	$N_{\text{found gr}}$, $\omega_0 = 10°$	n_{bound}	$N_{\text{found gr}}$, $\omega_0 = 5°$	$N_{\text{found gr}}$, $\omega_0 = 10°$
57	**2.00**	**745 (74)**	**659 (55)**	**100**	**741**	**682**
45	1.61	812 (87)	720 (65)	113	795	731
40	1.46	849 (91)	749 (63)	107	824	752
35	1.29	896 (125)	778 (87)	160	849	777
30	1.14	933 (133)	809 (90)	182	883	808
25	**1.00**	**963 (143)**	**814 (93)**	**195**	**898**	**823**
20	0.88	1011 (184)	862 (134)	225	920	842
15	0.75	1059 (210)	886 (139)	255	944	865
10	0.58	1149 (278)	951 (195)	325	957	873
8	**0.50**	**1203 (330)**	**958 (219)**	**383**	**970**	**890**

Relative Error $\delta_{\text{av.size}}$ of the Average Grain Size

• $\delta_{\text{less }h}$ is the fraction of grains in the specimen with sizes smaller than h.

A plus or minus indicates whether or not the chi-square homogeneity test for GSDD holds at 95 confidence level.

Table A.3

$\delta_{\text{less }h}$, %	Specimen (1)			Specimen (2)		
	h, μm	$\delta_{\text{av.size}}$, % $\omega_0 = 5°$	$\delta_{\text{av.size}}$, % $\omega_0 = 10°$	h, μm	$\delta_{\text{av.size}}$, % $\omega_0 = 5°$	$\delta_{\text{av.size}}$, % $\omega_0 = 10°$
57	**2.00**	**35.0 (–)**	**46.5 (–)**	**4.00**	**19.0 (+)**	**29.8 (–)**
45	1.61	25.8 (–)	36.8 (+)	3.54	13.2 (+)	24.2 (–)
40	1.46	21.3 (+)	33.0 (+)	3.38	10.4 (–)	20.7 (–)
35	1.29	17.8 (–)	28.7 (+)	3.24	9.0 (+)	18.5 (–)
30	1.14	13.2 (+)	23.7 (–)	3.09	7.6 (+)	18.0 (–)
25	**1.00**	**11.3 (+)**	**21.5 (+)**	**3.00**	**7.0 (+)**	**16.8 (+)**
20	0.88	8.7 (+)	18.7 (+)	2.70	4.0 (–)	14.0 (+)
15	0.75	6.0 (+)	15.6 (+)	2.52	3.3 (+)	13.0 (–)
10	0.58	4.5 (+)	14.5 (+)	2.30	2.5 (+)	12.2 (+)
8	**0.50**	**3.1 (+)**	**12.3 (+)**	**2.20**	**2.2 (–)**	**11.7 (+)**

Table A.4

$\delta_{\text{less } h}$, %	h, μm	Specimen (1) with boundaries		Specimen (1)	
		$\delta_{\text{av.size}}$, % $\omega_0 = 5°$	$\delta_{\text{av.size}}$, % $\omega_0 = 10°$	$\delta_{\text{av.size}}$, % $\omega_0 = 5°$	$\delta_{\text{av.size}}$, % $\omega_0 = 10°$
57	**2.00**	**34.2 (+)**	**51.7 (–)**	**35.0 (–)**	**46.5 (–)**
45	1.61	23.0 (+)	38.7 (–)	25.8 (–)	36.8 (+)
40	1.46	17.7 (+)	33.4 (–)	21.3 (+)	33.0 (+)
35	1.29	11.5 (+)	28.4 (–)	17.8 (–)	28.7 (+)
30	1.14	7.1 (+)	23.5 (–)	13.2 (+)	23.7 (–)
25	**1.00**	**3.8 (+)**	**22.8 (–)**	**11.3 (+)**	**21.5 (+)**
20	0.88	–1.1 (+)	16.0 (–)	8.7 (+)	18.7 (+)
15	0.75	–5.6 (+)	12.8 (–)	6.0 (+)	15.6 (+)
10	0.58	–13.0 (+)	5.1 (–)	4.5 (+)	14.5 (+)
8	**0.50**	**–17.0 (+)**	**4.4 (–)**	**3.1 (+)**	**12.3 (+)**

Variance of the Grain Size Distribution

- *Dx* is the variance of the grain sizes in the specimen.

Table A.5. Specimen (1)

$Dx = 1.688$			
h, μm	ω_0		
	20°	10°	5°
2.0	13.484	2.645	1.551
1.0	10.891	2.561	1.657
0.5	9.315	2.587	1.759

Table A.6. Specimen (1) with boundaries

$Dx = 1.688$			
h, μm	ω_0		
	20°	10°	5°
2.0	20.898	3.985	1.712
1.0	15.895	3.370	1.800
0.5	16.932	3.710	2.035

Variance of the Disorientation Angle Distribution between Grains

- $D\omega$ is the variance of disorientation angles in the specimen.

Table A.7. Specimen (1)

$D\omega = 0.031$			
h, μm	ω_0		
	20°	10°	5°
2.0	1.167	0.061	0.047
1.0	1.127	0.052	0.030
0.5	1.133	0.036	0.030

Table A.8. Specimen (1) with boundaries

$D\omega = 0.031$			
h, μm	ω_0		
	20°	10°	5°
2.0	0.189	0.105	0.086
1.0	0.217	0.114	0.102
0.5	0.421	0.256	0.227

REFERENCES

1. A. J. Schwartz, M. Kumar, B. L. Adams, and D. P. Field, *Electron Backscatter Diffraction in Materials Science*, 2nd. ed. (Springer, New York, 2009).
2. V. N. Danilenko, S. Yu. Mironov, A. N. Belyakov, and A. P. Zhilyaev, "Application of EBSD analysis in material science (overview)," Zavod. Lab. Diagn. Mater. **78** (2), 28–46 (2012).
3. F. J. Humphreys, "Grain and subgrain characterization by electron backscatter diffraction," J. Mater. Sci. **36**, 3833–3854 (2001).
4. S. Yu. Mironov, V. N. Danilenko, M. M. Myshlyaev, and A. V. Korneva, "Analysis of the spatial orientation distribution of building blocks in polycrystalline as determined using transmission electron microscopy and a backscattered electron beam in a scanning electron microscope," Phys. Solid State **47** (7), 1258–1266 (2005).
5. G. Gottstein, *Physical Foundations of Material Science* (Springer, New York, 2004; Binom, Moscow, 2009).
6. S. Zaefferer, "Application of orientation microscopy in SEM and TEM for the study of texture formation during recrystallization processes," *Proceedings of the 14th International Conference on Textures of Materials, ICOTOM 14* (Leuven, Belgium, 2005), pp. 213–128.
7. F. J. Humphreys, "Review grain and subgrain characterization by electron backscatter diffraction," J. Mater. Sci. **36**, 3833–3854 (2001).
8. V. Randle, "Electron backscatter diffraction: Strategies for reliable data acquisition and processing," Mater. Character. **60**, 913–922 (2009).
9. T. I. Savyolova, T. M. Ivanova, and M. V. Sypchenko, *Methods for Solving Ill-Posed Problems in Texture Analysis and Their Applications* (Mosk. Inzh.-Fiz. Inst., Moscow, 2012) [in Russian].
10. E. Guilmeau, C. Henrist, T. S. Suzuki, Y. Sakka, D. Chateigner, D. Grossin, and B. Ouladiaf, "Texture of alumina by neutron diffraction and SEM-EBSD," *Proceedings of the 14th International Conference on Textures of Materials, ICOTOM 14* (Leuven, Belgium, 2005), pp. 179–184.
11. N. Bozzolo, F. Gerspach, G. Sawina, and F. Wagner, "Accuracy of orientation distribution function determination based on EBSD data: A case study of a recrystallized low alloyed Zr sheet," J. Microscopy **227**, 275–283 (2007).
12. T. I. Savyolova and M. V. Sypchenko, "Calculation of the orientation distribution function from a set of individual orientations on $SO(3)$," Comput. Math. Math. Phys. **47** (6), 970–982 (2007).
13. K. P. Aganin and T. I. Savyolova, "Error estimates for kernel and projection methods of recovering the orientation distribution function on $SO(3)$," Comput. Math. Math. Phys. **48** (6), 1024–1038 (2008).

14. T. I. Savyolova and M. V. Sypchenko, "Error estimation of grain distribution function recovery for dependent orientations with allowance for grain sizes," Comput. Math. Math. Phys. **49** (5), 846–856 (2009).
15. K. N. Roginskii and T. I. Savyolova, "Polar figure computation by a kernel method from a set of individual grain orientations on *SO*(3)," Comput. Math. Math. Phys. **50** (5), 900–916 (2010).
16. S. Piazolo, V. G. Sursaeva, and D. J. Prior, "Optical grain size measurements: What is being measured? Comparative study of optical and EBSD grain size determination in 2D Al foil," *Proceedings of the 14th International Conference on Textures of Materials, ICOTOM 14* (Leuven, Belgium, 2005), pp. 213–218.
17. M. V. Sypchenko and T. I. Savyolova, "Some problems of measurement of individual grain orientations and computation of averaged elastic properties of magnesium," Zavod. Lab. Diagn. Mater., No. 6, 39–44 (2010).
18. M. V. Sypchenko and T. I. Savyolova, "Investigation of the accuracy of modeling the orientation distribution function of polycrystalline materials from individual orientations," Cristallogr. Rep. **55** (4), 546–550 (2010).
19. A. H. Zewail and J. M. Thomas, *4D Electron Microscopy: Imaging in Space and Time* (Imperial College Press, London, 2009; Intellekt, Dolgoprudnyi, 2013).
20. M. V. Borovkov and T. I. Savyolova, "Computation of normal distributions on rotation groups by the Monte Carlo method," Comput. Math. Math. Phys. **42** (1), 108–124 (2002).
21. M. Borovkov and T. I. Savyolova, "The computational approaches to calculate normal distributions on the rotation group," Mag. Appl. Cristallogr. **40**, 449–455 (2007).
22. S. A. Aivazyan and B. C. Mkhitaryan, *Applied Statistics and Basics of Econometrics* (YuNITI-DATA, Moscow, 2001) [in Russian].
23. software channel 5, www.hkltechnology.com
24. T. I. Savyolova, *Monte Carlo Method* (Mosk. Inzh.-Fiz. Inst., Moscow, 2011) [in Russian].
25. A. A. Natan, O. G. Gorbachev, and S. A. Guz, *Mathematical Statistics* (MZ Press, Moscow, 2004) [in Russian].

Translated by I. Ruzanova